Tectonophysics xxx (2013) xxx–xxx

Contents lists available at ScienceDirect

Tectonophysics

journal homepage: www.elsevier.com/locate/tecto

Spatial variations of seismic attenuation and heterogeneity in the Pyrenees: Coda *Q* and peak delay time analysis

Marie Calvet [a,*], Matthieu Sylvander [a], Ludovic Margerin [a], Antonio Villaseñor [b]

[a] IRAP, CNRS, Université de Toulouse, Observatoire Midi-Pyrénées, 14 Avenue Edouard Belin, F-31400 Toulouse, France
[b] Institute of Earth Sciences Jaume Almera, ICTJA-CSIC, Lluis Sole i Sabaris s/n, 08028 Barcelona, Spain

ARTICLE INFO

Article history:
Received 10 April 2013
Received in revised form 26 August 2013
Accepted 29 August 2013
Available online xxxx

Keywords:
Seismic attenuation
Coda waves
Wave scattering
Heterogeneity
Pyrenees

ABSTRACT

Lateral variations of seismic attenuation in the Pyrenees are explored from the analysis of local earthquake records. Scattering loss and intrinsic absorption both control the propagation of short period S waves through the crust. The role of intrinsic and scattering attenuation is analyzed in two steps. Firstly, the coda quality factor Q_c, which quantifies the energy decay of coda waves, is estimated at large lapse time in five frequency bands and interpreted as intrinsic absorption. Next, we systematically measure the peak delay time defined as the time lag from the direct S-wave onset to the maximum amplitude arrival. This parameter quantifies the strength of multiple forward scattering due to random inhomogeneities along the seismic ray path. Comparison of coda-*Q* and peak delay time measurements allows a qualitative interpretation of the origin of seismic attenuation (scattering/absorption) in the Pyrenean crust.

At low frequency, coda-*Q* variations mainly depend on the tectonic units of the Pyrenees, with stronger absorption in sedimentary basins and smaller absorption in Paleozoic basements. At high frequency, coda-*Q* is low at the location of Neogene structures in the Eastern Pyrenees. A more enigmatic low-Q_c anomaly is also observed at the location of the Maladeta Massif in the Central Pyrenees. In all frequency bands, peak delay time measurements systematically show stronger scattering in the Western Pyrenees.

In the Labourd–Mauléon area, absorption and scattering are both important at low frequency. The Western Pyrenees also correspond to a high-velocity/density anomaly revealed from tomography and gravity data analysis. This suggests that the high level of inhomogeneities and absorption may be related to intrusion of mantle and/or lower-crustal materials. In the Eastern Pyrenees, absorption appears dominant over scattering at high frequency. We hypothesize that the strong absorption observed in this area may be related to volcanic structures.

1. Introduction

In complement to seismic velocity measurements, attenuation provides valuable informations about the structure of the Earth. It is also an important parameter for the quantitative evaluation of earthquake ground motion. Three mechanisms can be invoked to explain seismic wave attenuation: (1) anelastic absorption which mainly depends on temperature, melt or fluid content, and chemical composition, (2) scattering of seismic waves generated by small-scale velocity fluctuations and (3) focusing due to propagation in 3-D structures. The separation of these different effects is still a significant challenge but various methods have been proposed to estimate the relative contribution of anelasticity and scattering to the seismic attenuation in the Earth lithosphere (see Sato et al., 2012, for a review).

Substantial regional variations in the attenuation of high-frequency seismic waves have been documented in several studies (see Romanowicz and Mitchell, 2007, for a review). Few studies have explored the seismic attenuation in the French lithosphere (e.g. Campillo and Plantet, 1991; Campillo et al., 1985; Chevrot and Cansi, 1996; Lacombe et al., 2003), but some of them have detected differences between distinct tectonic units. For example, attenuation at 1 Hz may be stronger in the Alps than in the Pyrenees (Drouet et al., 2008, 2010). In Spain, Pujades et al. (1990) and Payo et al. (1990) have shown that seismic attenuation at 1 Hz may be higher in the Pyrenees than in Galicia or in the Ebro Basin. But only a few studies specifically concern the Pyrenees. These studies either focus on a specific area (Correig et al., 1990; Gagnepain-Beyneix, 1987) or propose an estimation of the seismic attenuation for the entire Pyrenean range (Calvet and Margerin, 2013; Drouet et al., 2005). However, there is some evidence of strong lateral variations of both seismic absorption and scattering properties in the Pyrenees, as illustrated by the L_g blockage phenomenon observed in the western part of the range (Chazalon et al., 1993; Sens-Schönfelder et al., 2009).

Because of easy applicability, many determinations of seismic attenuation have involved so far the use of coda waves of local earthquakes.

* Corresponding author. Tel.: +33 561333014.
E-mail address: Marie.Calvet@irap.omp.eu (M. Calvet).

0040-1951/$ – see front matter © 2013 Elsevier B.V. All rights reserved.
http://dx.doi.org/10.1016/j.tecto.2013.08.045

Coda Q measurements (noted Q_c hereafter) was extensively used in seismology for lithospheric or crustal attenuation studies (Aki and Chouet, 1975; Mitchell, 1995; Sato et al., 2012). However Q_c depends simultaneously on the scattering and anelastic properties of the crust. By using the MLTWA method developed by Fehler et al. (1992), Carcolé and Sato (2010) have recently obtained high resolution maps of scattering and intrinsic attenuation for Japan. They also demonstrated that the spatial variations of intrinsic absorption and Q_c are highly correlated. In complement to coda Q measurements, analyses of high-frequency seismic envelopes have been used to discuss the relative contribution of intrinsic absorption and scattering loss to the total seismic attenuation (Obara and Sato, 1995; Petukhin and Gusev, 2003; Saito et al., 2002, 2005; Sato, 1989; Takahashi et al., 2007). Multiple scattering due to random velocity inhomogeneities increases the apparent duration of the S-wave pulse. On the contrary, intrinsic absorption truncates it. The seismic wave envelope results from a competition between scattering and absorption (Saito et al., 2005).

In this study, we propose to explore more systematically the regional variations of Q_c and pulse broadening in order to discuss the origin (scattering and/or absorption) of the lateral variations of seismic attenuation in the Pyrenees. To characterize the spatial variations of attenuation in the Pyrenees, we take advantage from a dense seismic network. Several institutes in France and Spain operate about 70 permanent seismic stations in the Pyrenees, and two temporary experiments have been conducted since 2010 on both sides of the mountain range. The paper is organized as follows. First, we summarize the main tectonic and seismological structures of the Pyrenees (Section 2). Then, we present our data set in Section 3. Coda-Q and pulse broadening measurements are discussed in Sections 4 and 5, respectively. The origin of the observed spatial variations of both observables is discussed in Section 6. Conclusions are given in Section 7.

2. Structure of the Pyrenees

2.1. Seismotectonic settings

The Pyrenees are an asymmetrical, double-wedge continental belt about 400 km long and 150 km wide which exhibits a North–South structure described by three main tectonic units: the Paleozoic Axial Zone (PAZ), the North Pyrenean Zone (NPZ) and the South Pyrenean Zone (SPZ) (Choukroune, 1992). These principal units are shown in Fig. 1. The North Pyrenean Fault (NPF) is the major tectonic feature in the Pyrenees. It is observed at the surface in the central and eastern parts of the range. The NPF is also characterized by metamorphic rocks and lherzolite outcrops (Lagabrielle and Bodinier, 2008). Other important fault systems are the Adour fault with a NW–SE orientation in the Central Pyrenees, and the Têt and Tech faults in Eastern Pyrenees. Intricate fault systems related to the Western Mediterranean opening are observed at the southeast end of the Pyrenees and in the Catalan Coastal Ranges. The PAZ is largely inherited from Hercynian structures and includes several granitic massifs such as the Maladeta Massif. It also includes the highest summits. The NPF marks the boundary between the PAZ and the NPZ. The NPZ corresponds to the former Eurasian margin thinned during the Cretaceous extension phase. It is mainly composed of highly deformed Mesozoic flysh deposits. It also includes large Paleozoic outcrops such as the North Pyrenean Massifs in the central part of the range (noted NPM in Fig. 1) and the Basque Massifs to the west. To the north, the NPZ sediments override the Aquitaine Basin along the North Pyrenean Frontal Thrust. To the south, the South Pyrenean Zone (SPZ) is composed of Mesozoic and Cenozoic sediments which overthrust the molasse of the Ebro Basin.

The Pyrenees have been affected by several successive orogens. From 120 to 80 Ma, the Pyrenean domain and the Hercynian structures

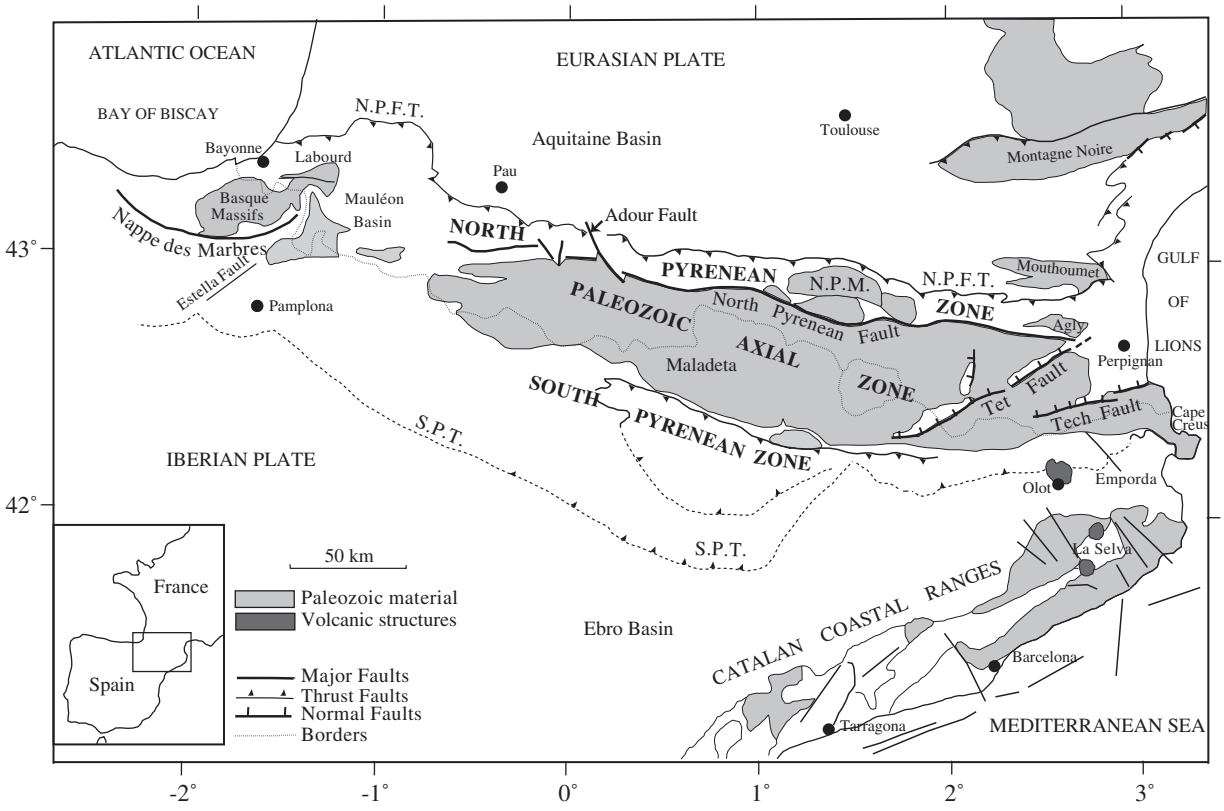

Fig. 1. Main structural units of the Pyrenees after Choukroune (1992). NPFT: North Pyrenean Frontal Thrust; NPM: North Pyrenean Massifs; SPT: South Pyrenean Thrust. Light gray zones correspond to Paleozoic material while dark gray zones indicate Quaternary volcanic rocks.

Please cite this article as: Calvet, M., et al., Spatial variations of seismic attenuation and heterogeneity in the Pyrenees: Coda Q and peak delay time analysis, Tectonophysics (2013), http://dx.doi.org/10.1016/j.tecto.2013.08.045

experienced an extension episode related to the opening of the Bay of Biscay with the rotation of the Iberian plate. During this episode, the crust was thinned and affected by dense lower crust and upper mantle intrusions in the western and central part of the Pyrenees. Two competing plate-kinematic models have been proposed to describe the rotation of Iberia with respect to Europe: a scissor-type opening model (Rosenbaum et al., 2002; Srivastava et al., 2000) or a left-lateral strike-slip opening model (Jammes et al., 2009; Le Pichon and Sibuet, 1971). Recently, Vissers and Meijer (2012) have proposed a third geodynamical scenario consistent with both seafloor magnetic anomaly data and geological observations: during the progressive opening of the Bay of Biscay, the mantle lithosphere subducted and became gravitationally unstable leading to asthenospheric upwelling with magmatism and metamorphism. The second stage for the formation of the Pyrenees is the North–South collision of the Eurasian and Iberian plates about 65 Ma ago, with less shortening in the Western Pyrenees than in the Central Pyrenees (Vergés et al., 2002). The Eastern Pyrenees also experienced Neogene extension during the rotation of the Corsica–Sardinia block. Neogene to Quaternary volcanism has affected the Catalan Coastal Ranges and the south-eastern Pyrenees in the Olot region (Martí et al., 1992).

The seismic activity of the Pyrenees is known from historical catalogs as well as from instrumental seismological studies. The present-day seismicity in the Pyrenees is moderate with an average of one event per year with a magnitude greater than 4 (Rigo et al., 2005; Ruiz et al., 2006; Souriau and Pauchet, 1998). The geographical distribution of Pyrenean earthquakes is very inhomogeneous. To the west, a diffuse activity is observed in the southern part of the range around Pamplona. In the Central Pyrenees, the seismicity is mostly in the North Pyrenean Zone but without any clear evidence of relationship with the surface location of the NPF (Rigo et al., 2005; Souriau et al., 2001). The seismicity becomes much more diffuse in the eastern part of the Pyrenees with a clear southward shift of the seismicity. The current tectonic regime in the Pyrenees still remains uncertain (Nocquet and Calais, 2004; Rigo et al., 2005; Souriau et al., 2001) even if most of the recent significant earthquakes exhibit East–West extensional fault plane solutions more particularly in the Central Pyrenees (Chevrot et al., 2011).

2.2. Seismic structure of the Pyrenean crust

Crustal structures in the Pyrenees have been widely explored using seismic and gravity data. Geophysical studies based on refraction and ECORS deep penetration seismic profiles (Choukroune et al., 1990) show a large Moho jump along the NPF. The crust is much thicker on the Iberian side (50–55 km) than on the French side (28–30 km). From refraction profiles, there is some evidence that the crust south of the NPF has a 50 km maximal thickness beneath the center of the range, and is progressively thinned to 23 km to the East (Gallart et al., 1981; Mauffret et al., 2001) and to 40 km to the West (Gallart et al., 1980, 2001). The lower crust in the western part of the NPZ displays much higher P wave velocity than in the PAZ likely due to mantle intrusions into the lower crust (Daignieres et al., 1981).

The crustal seismic tomography by Souriau and Granet (1995) has revealed two high-velocity bodies (both for P waves and S waves) in the Central and Western parts of the North Pyrenean Zone (Fig. 2a). These two fast seismic anomalies also correspond to high density bodies (Casas et al., 1997; Jammes et al., 2010; Vacher and Souriau, 2001) as suggested by positive Bouguer anomalies (Fig. 2c). Such gravity anomalies could be related to lower crust or mantle materials that were uplifted at shallower depth and possibly exhumed during Early Cretaceous rifting before being integrated to the Pyrenean range during the collision phase (Jammes et al., 2009, 2010; Vacher and Souriau, 2001). In Fig. 2b, we also show the mean crustal V_P/V_S ratio computed at several seismic monitoring stations from Wadati diagrams. We observe that Paleozoic materials are characterized by rather low V_P/V_S ratios whereas the Mauléon Basin, Pamplona Basin and the SPZ (in Central Pyrenees) exhibit larger V_P/V_S values. In contrast, the seismic attenuation structure of the Pyrenean crust is relatively poorly known. Recently, Sens-Schönfelder et al. (2009) and Calvet and Margerin (2013) have shown that absorption may be slightly dominant over scattering at low frequency with probably some lateral variations. In particular, scattering and absorption may be significantly stronger in the Western Pyrenees than in the surrounding regions (Sens-Schönfelder et al., 2009).

3. Data selection

In this study, we analyze velocity waveform data recorded by permanent and temporary seismic networks in the Pyrenees. We collect around 10,000 waveform data recorded at 117 stations from 741 earthquakes which occurred between 2001 and 2011, with a local magnitude (*ML*) larger than 2.0. Focal depths vary between 1 km and 20 km. Location of epicenters, local magnitude and origin time of earthquakes have been determined by the Réseau de Surveillance Sismique des Pyrénées (RSSP). Our dataset mainly contains short period velocimetric waveforms from RSSP (20 stations). We also include accelerometric data from RAP (Réseau Accélérométrique Permanent — 23 stations) and IGC (Institut Geològic de Catalunya — 13 stations), and broadband velocimetric data from IGC (14 stations) and IGN (Instituto Geogràfico Nacional — 8 stations). These data have been collected in the framework of the European project SISPYR (http://www.sispyr.eu). We also selected a few broadband records from the PYROPE (http://w3.dtp.obs-mip.fr/RSSP/PYROPE/) and IBERARRAY (http://iberarray.ictja.csic.es) experiments which have been deployed in the Pyrenees at the end of 2010. Most of the short period velocimetric and accelerometric data are recorded by triggered systems whereas broadband stations record continuously. Locations of epicenters and stations are reported in Fig. 3. Epicentral distances range from 1 km to 400 km.

4. Coda *Q* observations

4.1. Definition of coda Q

Aki and Chouet (1975) have observed that the energy envelope of seismic coda waves decays as:

$$E(t,f) = S(f)t^{-\alpha}e^{-2\pi ft/Q_c(f)} \quad (1)$$

where E is the power spectral density, $S(f)$ is a frequency-dependent source and/or site term, t is the lapse time, f is the frequency, α is a positive exponent, and Q_c is the frequency-dependent quality factor of coda waves. It is well documented that independent estimates of Q_c and α cannot be achieved from data only. Therefore, the value of α must be fixed a priori, but the impact on the estimated Q_c value is typically less than 20% (Aki and Chouet, 1975). The value of α and the interpretation of the coda quality factor Q_c depend on the physical model used to describe coda waves. A single-scattering interpretation of the seismic coda in a homogeneous half-space is compatible with Eq. (1) for an exponent α equal to 2. In that case, the coda quality factor Q_c depends simultaneously on the scattering and absorption as follows (Sato et al., 2012):

$$Q_c^{-1} = Q_{sc}^{-1} + Q_i^{-1} \quad (2)$$

where Q_{sc} and Q_i are the scattering and intrinsic absorption quality factor, respectively. However, the observation of seismic wave equipartition puts forward the role of multiple scattering in the generation of coda waves (Hennino et al., 2001). For example, in the Central Pyrenees, Souriau et al. (2011) have demonstrated that the equipartition regime may be reached only a few seconds after the S-wave onset. Within the multiple scattering interpretation of coda waves, the physical meaning of Q_c is radically different.

Please cite this article as: Calvet, M., et al., Spatial variations of seismic attenuation and heterogeneity in the Pyrenees: Coda Q and peak delay time analysis, Tectonophysics (2013), http://dx.doi.org/10.1016/j.tecto.2013.08.045

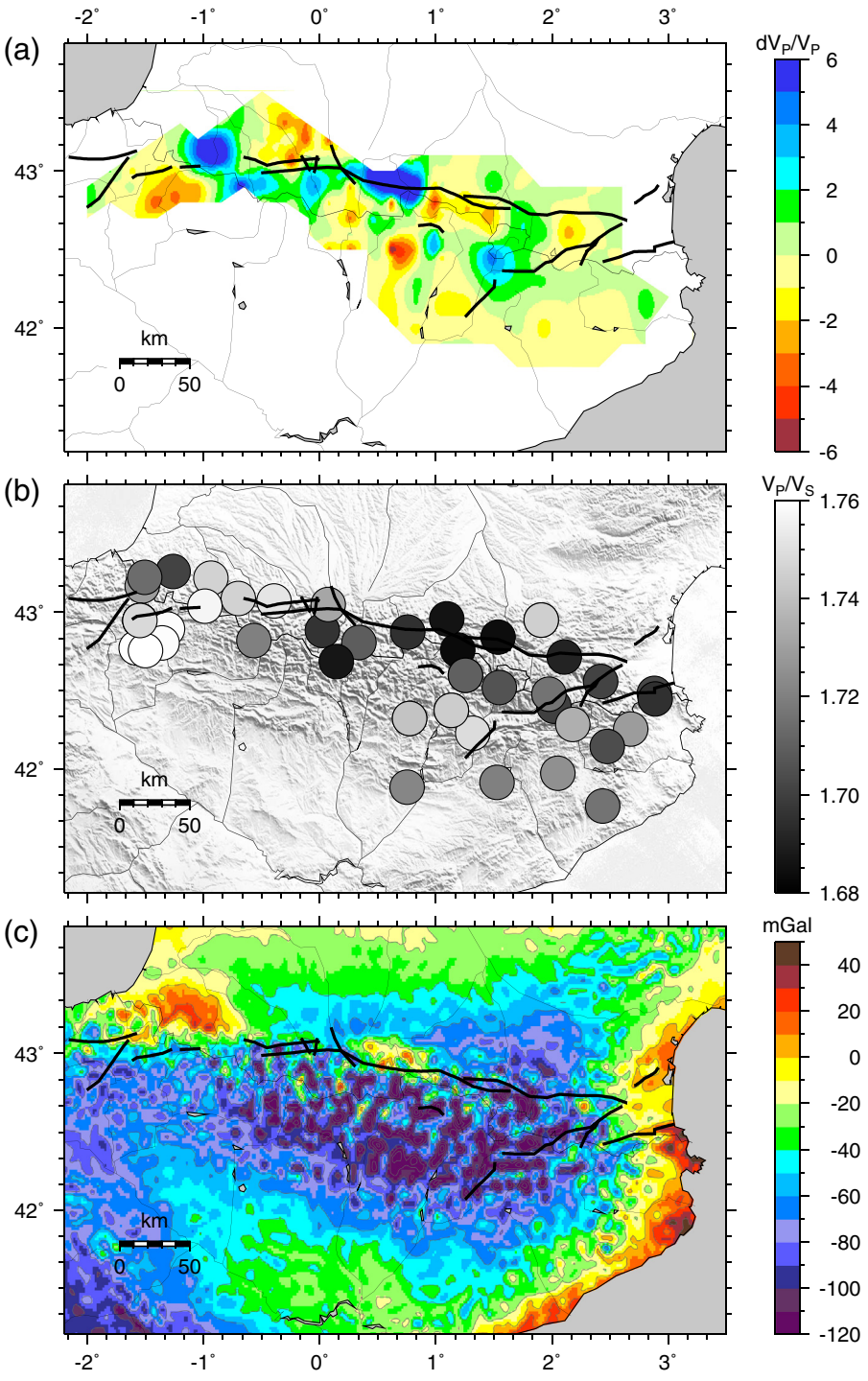

Fig. 2. (a) Crustal P-wave tomographic model by Souriau and Granet (1995) at depth 11 km. (b) V_P/V_S ratio computed at some French and Spanish velocimeter stations. (c) Bouguer anomalies (computed by International Gravimetric Bureau — http://bgi.omp.obs-mip.fr/). Black thick lines are the main Pyrenean faults.

After a few mean free times, multiple-scattered waves reach a diffusion regime which implies that

$$Q_c = Q_i \tag{3}$$

in a uniform half-space (Sato et al., 2012). In the present study, we adopt a multiple scattering interpretation of Q_c with $\alpha = 3/2$ in Eq. (1) (Paasschens, 1997).

4.2. Q_c measurement methodology

Prior to estimating the power spectral density $E(t,f)$ at lapse time t in the coda, we deconvolve the waveform from the station response and accelerometer records are integrated to get the vertical component of velocity. For Q_c measurements, only events with a local magnitude greater than 2.5 are processed. Using a bandpass Butterworth filter of order 4, data are filtered in five frequency bands: 1–2 Hz, 2–4 Hz, 4–8 Hz, 8–16 Hz, and 16–32 Hz. In each frequency band, we smooth the

Please cite this article as: Calvet, M., et al., Spatial variations of seismic attenuation and heterogeneity in the Pyrenees: Coda Q and peak delay time analysis, Tectonophysics (2013), http://dx.doi.org/10.1016/j.tecto.2013.08.045

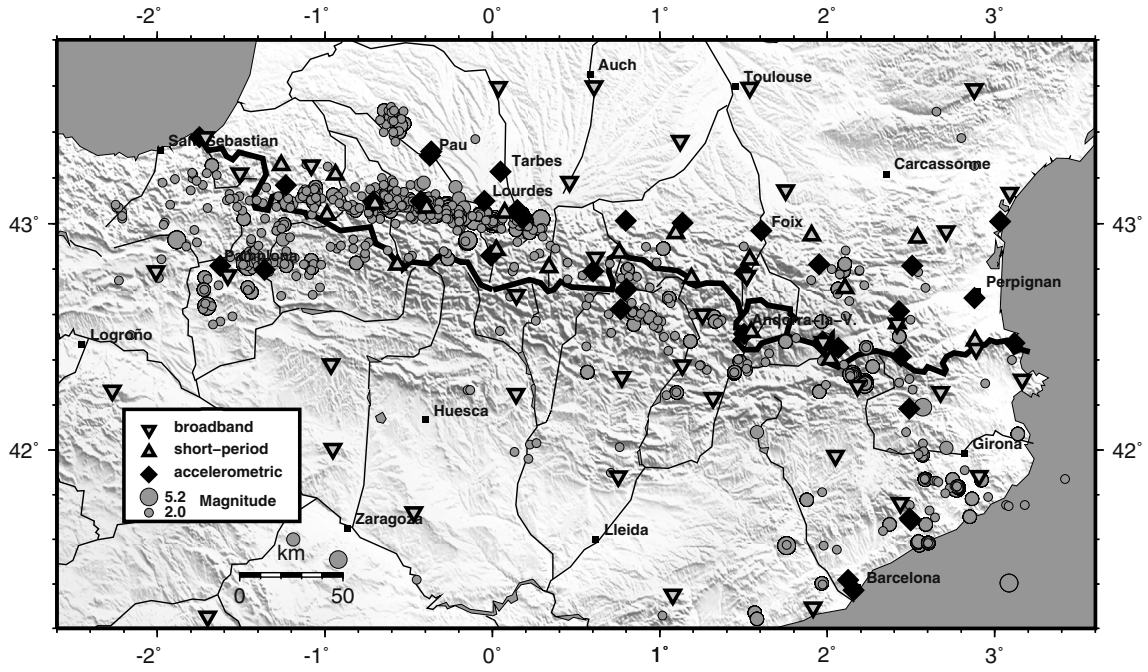

Fig. 3. Location map of earthquakes and seismological stations used for coda-Q and peak delay time measurements. See inset for symbol explanation.

squared vertical traces with a moving window whose typical duration is of the order of 16 cycles. The smoothed envelopes are thus corrected for the algebraic terms $t^{-3/2}$. In each frequency band, an estimate of Q_c is obtained from a least-square linear fit of $E(t,f)t^{3/2}$ as a function of t in a coda window of duration L_W starting at a lapse time t_W (from the origin time of the earthquake). The values of Q_c are accepted when the signal-to-noise ratio is greater than 4 and the correlation coefficient of the linear regression is greater than 0.7.

4.3. Lapse-time and frequency dependence of Q_c

In Fig. 4, we represent all estimates of Q_c in the frequency band 4–8 Hz as a function of epicentral distance. The coda window length is fixed at $L_W = 30$ s and three possible choices of coda onset t_W are explored: (a) $t_W = 2t_s$ – commonly adopted in the seismological literature – where t_s is the ballistic time of S wave in the crust, (b) $t_W =$ 50 s after the origin time of the earthquakes, and (c) $t_W = 80$ s. The purpose of this plot is to identify the range of epicentral distances and lapse time which allow stable measurement of Q_c. For $t_W = 2t_s$, Q_c increases with epicentral distance ($R \leq 100$ km) and reaches a plateau value of ~ 800 ± 250 at large epicentral distances ($R > 100$ km). For $t_W = 50$ s, Q_c is almost independent of distance for $R \leq 100$ km, with an amplitude close to 800, and decreases rapidly at larger epicentral distances. At sufficiently large t_W (80 s, Fig. 4c), Q_c is stable (800 ± 250) throughout the epicentral distance range we have explored.

The choice of coda window is thus crucial to map the lateral variations of seismic attenuation. If different coda windows are mixed (early and late coda window), it may happen that the lateral variations of Q_c are measurement artifacts. For a selected range of epicentral distances, we must fix the coda onset t_W and the coda window length L_W, to facilitate the physical interpretation of Q_c. In particular, we must be sure that its estimate is not hampered by the transient regime occurring at short lapse time (Calvet and Margerin, 2013). However the number of signals which allow measurements at sufficiently large lapse time is limited by the length of the triggered seismic records and by the noise level. The best compromise is to measure Q_c in the five frequency bands for epicentral distances smaller than 90 km and for a 30 s coda window starting 50 s after the origin time of the earthquakes. This range of parameters corresponds to the plateau apparent in Fig. 4b (for the frequency band 4–8 Hz). Our choice of coda window allows good spatial coverage of the Pyrenees and ensures that Q_c provides a reliable estimate of the absorption quality factor Q_i at all frequency. As discussed by Calvet and Margerin (2013), absorption is to be understood as the combined effect of anelasticity and leakage (Margerin et al., 1999), the latter being negligible except in locally strongly scattering area. The range of fluctuations of Q_c (±250) around the plateau

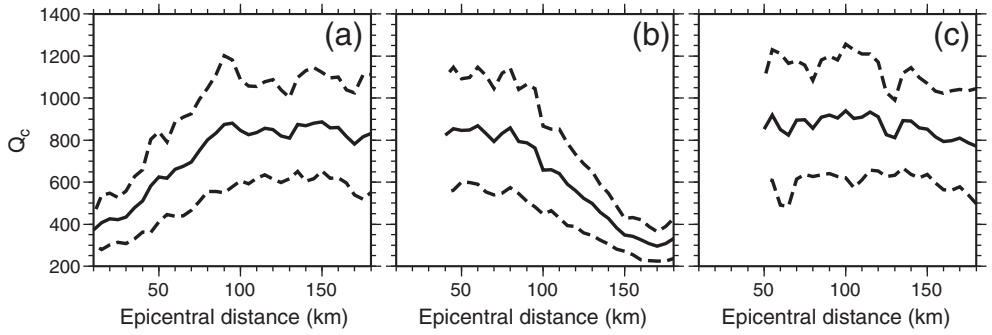

Fig. 4. Q_c as a function of the epicentral distance in the frequency band [4–8 Hz]. Solid line is the mean value and dashed lines correspond to one standard deviation. The coda windows start at $2t_s$ (a), 50 s (b), and 80 s (c) after the origin time of the earthquake. t_s is the S-wave travel time. The length of the coda window is fixed at 30 s.

Please cite this article as: Calvet, M., et al., Spatial variations of seismic attenuation and heterogeneity in the Pyrenees: Coda Q and peak delay time analysis, Tectonophysics (2013), http://dx.doi.org/10.1016/j.tecto.2013.08.045

value (~ 800 in the frequency band 4–8Hz) is typically one order of magnitude larger than the uncertainty of individual measurements. We can thus confidently propose that the fluctuations are due to strong variations of absorption properties along the Pyrenean range.

Adopting the selection criteria discussed above, the total numbers of Q_c measurements in the five frequency bands are: 2190 (1–2 Hz), 2260 (2–4 Hz), 2296 (4–8 Hz), 2293 (8–16 Hz), and 2035 (16–32 Hz). These measurements can be summarized by a simple power law of the form $Q_0 f^n$ where Q_0 is the value of Q_c at 1 Hz and n is an exponent which accounts for the frequency dependence. A simple fit yields $Q_0 = 220(\pm 84)$ and $n = 0.64 \pm 0.15$ for the Pyrenees. Previous studies have also reported a frequency dependence of Q_c in the Pyrenees. In the Western Pyrenees, on the western end of the Axial Zone, Gagnepain-Beyneix (1987) finds Q_0 and n in the range [30 — 140] and [0.7 — 1.1], respectively. In the Eastern Pyrenees, close to Andorra, Correig et al. (1990) obtain $Q_0 \sim 14$ and $n \sim 1.13$, indicating stronger attenuation at 1 Hz in the Western Pyrenees. These two studies focused on the analysis of nearby earthquakes (epicentral distances smaller than 40–30 km) using a coda window starting at $t_W = 2t_s$ which mostly samples the early coda. This choice of coda window may largely underestimate Q_c-values (see Fig. 4a) and cannot be easily interpreted in terms of absorption. On the contrary, our results are close to those of Mitchell et al. (2008) ($Q_0 \in [200 - 300]$ and $n \in [0.6 - 0.7]$) obtained at large lapse time.

4.4. Spatial distribution of Q_c in the Pyrenees

4.4.1. Mapping methodology

Usually, the classical quality factor regionalization approach adopted with coda waves considers that the sensitivity is distributed within ellipsoidal shells whose size increases with the lapse time in the coda (e.g. Mitchell, 1995; Mitchell et al., 2008; Vargas et al., 2004). Recent progresses in the modeling of seismic coda waves challenge this view. In particular, in the multiple scattering regime, the coda wave sensitivity strongly depends on the type of perturbation (elastic or anelastic), and is not distributed within an ellipsoid. In diffusive propagation model, it has been verified that the coda waveform sensitivity to slowness or scattering perturbation is larger at the locations of the source and the station (Pacheco and Snieder, 2005; Rossetto et al., 2011). The sensitivity kernels of coda wave intensity to local variations of absorption still have to be derived, but we expect similar spatial sensitivity. Consequently, we adopt a very simple Q_c regionalization approach which consists of assigning Q_c values to ray paths between stations and hypocentres. As the sensitivity of coda waves may be stronger near the station and the source, we should select Q_c measurements for rather small epicentral distances. We tested various epicentral distance ranges, but to preserve good spatial coverage in Q_c maps, we decided to select all the data for epicentral distance smaller than 90 km.

For simplicity, we only consider 2D lateral variations of Q_c. Seismic ray paths are calculated considering that the S-wave velocity is homogeneous (about 3.5 $km \cdot s^{-1}$). The depth distribution of hypocentres, indicates that most of the ray paths are located in the first 20 km of the crust. We divide the Pyrenean crust into rectangular $0.1^\circ \times 0.1^\circ$ blocks. As many ray paths propagate through one block and each ray path indicates a different value of Q_c, we propose to allocate the mean values of Q_c to each block. Only blocks crossed by at least 2 ray paths are retrieved. Finally, for each block, we take an average of the mean value over the nearest nine blocks to smooth the spatial variations.

4.4.2. Main characteristics of the Q_c maps

Fig. 5 shows the spatial distribution of Q_c and the ray path density in the five frequency bands. The spatial coverage of the Pyrenees is rather good, more particularly in areas characterized by a strong density of seismic stations and earthquakes. Strong absorption (small Q_c values) is indicated in red colors whereas low absorption (large Q_c values) is indicated in blue colors.

At low-frequency, we observe a rather good correlation between attenuation structures and the main tectonic units of the Pyrenees described by Choukroune (1992). In the 1–2 Hz map, Precambrian and Paleozoic basements in the Eastern (from NPF to the Catalan Coastal Range) and the Central Pyrenees (between the North Pyrenean Thrust and the southern limit of the PAZ) are characterized by smaller attenuation (larger Q_c values) than the South Pyrenean Zone, the Mauléon, Pau and Pamplona Basins. However, the Paleozoic Basque Massifs exhibit stronger attenuation than other Paleozoic structures of the Pyrenees. Q_c maps also reveal a North–South low-Q_c anomaly at the longitude of the Hercynian Maladeta Massifs (longitude 1.5°) which crosses the Pyrenees from the Aquitaine Basin to the Ebro Basin. On average, similar Q_c structures are observed in the 2–4 Hz map, except for the Mauléon Basin where attenuation becomes smaller than in the sediments of Pamplona and Pau Basins. In conclusion, our low-frequency Q_c maps are characterized by rather strong absorption in the Western Pyrenees and small absorption in the Eastern Pyrenees with in average stronger absorption in sedimentary structures than in Paleozoic materials.

At high frequency (>4 Hz), the Q_c pattern in the Pyrenees changes drastically and cannot be easily related to the principal tectonic units. The most striking feature is the low-Q_c anomaly clearly delimited by the Neogene structures (Olot and La Selva volcanic areas) in the Eastern Pyrenees. We also observe that the North–South low-Q_c anomaly already detected at low frequency spreads from the Maladeta Massif to the Adour Fault. Surprisingly, the sediments in Aquitaine and Ebro Basins as well as the Hercynian massifs of the Paleozoic Axial Zone in the Eastern Pyrenees exhibit similar seismic absorption. In the Westernmost Pyrenees, the strong attenuation anomaly is now limited to the Basque Massifs. We will discuss all these features in Section 6.

5. Peak delay time observations

5.1. Definition of the peak delay time

In randomly heterogeneous media, an impulsive seismic wave radiated from the source broadens as its travel distance increases. The broadening of energy envelopes with epicentral distance is a clear manifestation of multiple forward scattering in the Earth (Saito et al., 2002; Sato, 1989). Various delay-time definitions have been proposed in the literature to measure the envelope-broadening and to quantify the strength of multiple scattering due to random heterogeneities along the seismic ray path (e.g., Tripathi et al., 2010). For example, the peak delay time (noted T_{pd} hereafter and defined as the time lag from the S-wave onset to the maximum of the amplitude) has been mainly used to characterize the scattering properties of the Japanese lithosphere from high-frequency seismograms of local earthquakes with focuses deeper than the Moho (Obara and Sato, 1995; Saito et al., 2002, 2005; Sato, 1989; Takahashi et al., 2007, 2009). Envelope-broadening has been also observed from crustal event records in continent (North America) and subduction zones (Kamchatka, Japan) (Atkinson, 1993; Petukhin and Gusev, 2003; Tripathi et al., 2010).

In this study, we propose a first attempt at measuring and mapping the peak delay time T_{pd} in the Pyrenees.

5.2. T_{pd} measurements

We select data from permanent stations for earthquakes with a local magnitude greater than 2.0. We consider records with hypocentral

Fig. 5. Regional variations of Q_c (left) and ray path density (right). Q_c is estimated in five frequency bands from 1–2 Hz (top) to 16–32 Hz (bottom). Blocks with less than two measurements are shown in gray in Q_c maps. (For interpretation of the references to color in this figure, the reader is referred to the web version of this article.)

Please cite this article as: Calvet, M., et al., Spatial variations of seismic attenuation and heterogeneity in the Pyrenees: Coda Q and peak delay time analysis, Tectonophysics (2013), http://dx.doi.org/10.1016/j.tecto.2013.08.045

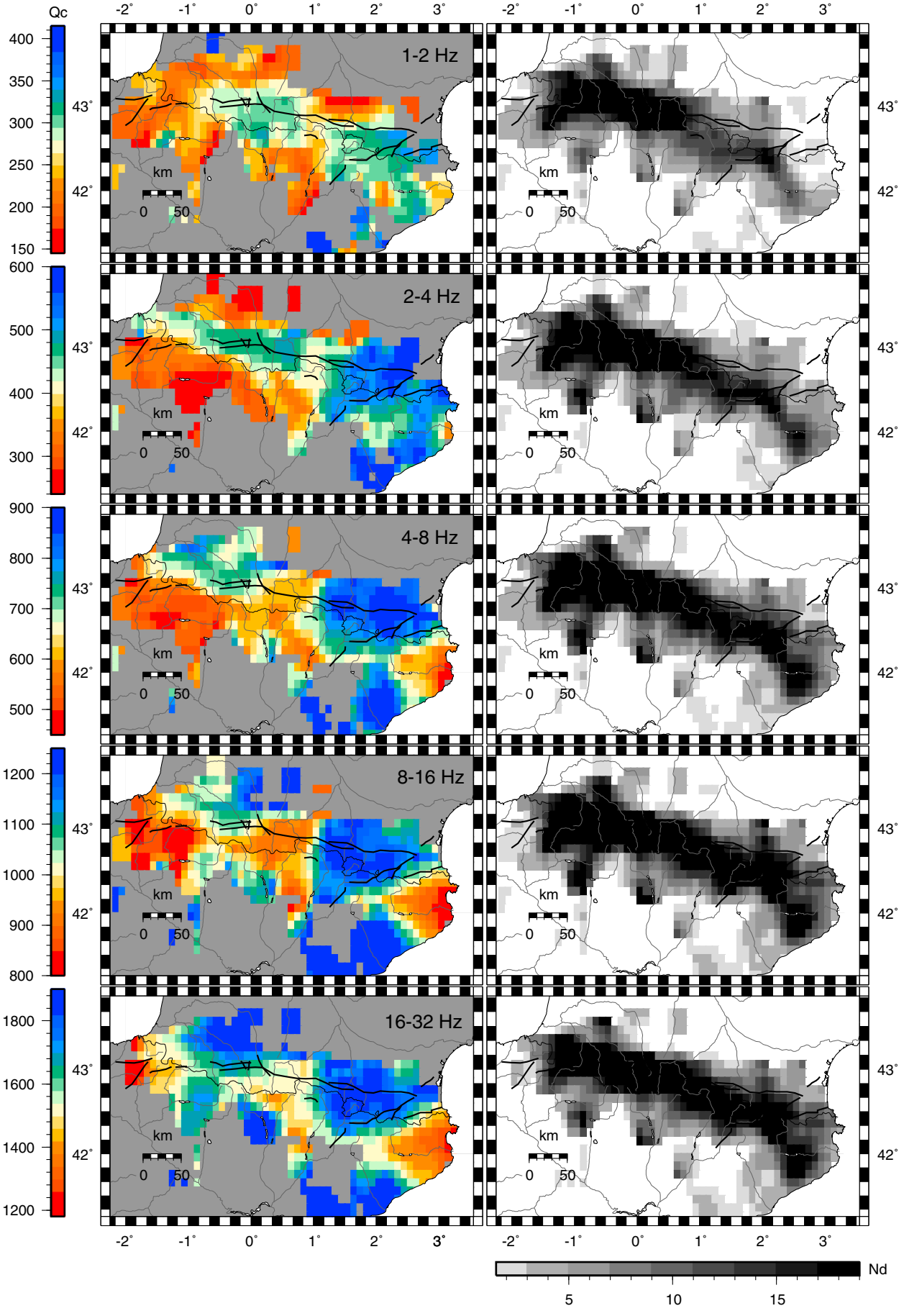

Please cite this article as: Calvet, M., et al., Spatial variations of seismic attenuation and heterogeneity in the Pyrenees: Coda Q and peak delay time analysis, Tectonophysics (2013), http://dx.doi.org/10.1016/j.tecto.2013.08.045

distances smaller than 80 km in order to focus on crustal phases only. The waveforms are first deconvolved from the recording system response. Seismograms are filtered in four frequency bands (2–4 Hz, 4–8 Hz, 8–16 Hz, 16–32 Hz) in forward and backward directions to avoid any phase delay caused by using the fourth-order bandpass Butterworth filter. Next, we compute the root mean square of the horizontal velocity components. The envelopes are smoothed with a moving time window whose typical duration is twice the central period of each frequency band. We only used waveform data which show a clear S-wave onset (quantified by the picking weight and measured on unfiltered records). S-wave onsets have been collected from local seismicity catalogs distributed by the institutes in charge of the seismic monitoring of the Pyrenees (RSSP, IGN and IGC). T_{pd} is measured in seconds in a 40 s time window starting at 0.5 s before the S-wave onset. Fig. 6 shows an example of T_{pd} measurements in the frequency band 4–8 Hz. We obtained 5157 T_{pd} measurements in each frequency band.

5.3. Hypocentral distance and frequency dependence of T_{pd}

Fig. 7 shows T_{pd} measurements (gray dots) as a function of the hypocentral distance R in the four frequency bands. Typically, at 80 km epicentral distance, the peak delay time can reach 4 s. Large values of T_{pd}, while absorption is also important (see previous section), reveal that scattering is rather strong in the Pyrenean crust. Black solid lines in Fig. 7 show the linear regression of $\log_{10}(T_{pd})$ against hypocentral distance $\log_{10}(R)$ by using the following equation:

$$\log_{10} T_{pd}(f) = A_r(f) + B_r(f)\log_{10} R. \quad (4)$$

The regression coefficients A_r and B_r and their standard deviations are given in Table 1. Although data are widely scattered, we observed that $\log_{10}(T_{pd})$ increases almost linearly with the logarithm of the hypocentral distance as previously observed in Japan for crustal and deep earthquakes (Takahashi et al., 2007; Tripathi et al., 2010).

The comparison of the linear regression coefficients in the frequency band 4–32 Hz reveals that T_{pd} slightly increases with frequency (at fixed hypocentral distance). Using the Markov approximation of the parabolic wave equation, Saito et al. (2002) have verified that envelope broadening strongly increases with frequency as the content of the random media in short-wavelength increases. Our measurements may thus suggest that the Pyrenean crust is poor in short-wavelength components, in agreement with (Calvet and Margerin, 2013) who have proposed that the inhomogeneity in the Pyrenees may be described by a Von-Karman random medium with a hurst exponent larger than 1. Alternatively, the frequency dependence of T_{pd} may be also related to the frequency dependence of absorption. Coda Q measurements at large lapse time indicate that the average absorption quality factor in the Pyrenees varies as $\approx 220 f^{0.64}$. Consequently, the absorption time decreases with frequency as $f^{-0.36}$. We hypothesize that the decrease of the absorption time with frequency hampers the broadening effect of small-scale heterogeneities and results in a slow increase of T_{pd} with frequency (Saito et al., 2002; Tripathi et al., 2010).

However, we should take into account that the model proposed by Saito et al. (2002) hypothesizes that the envelope-broadening is only due to scattering by lithospheric heterogeneities. This model is useful for the interpretation of high-frequency seismograms of deep earthquakes. For shallow earthquakes, envelope-broadening may also depend on the velocity structure. Indeed, in addition to scattering by random heterogeneities, the envelope-broadening of crustal phases may be strongly affected by multiple reflections in the crust, depth variations of the Moho and surface topography (e.g., Fu et al., 2002; Tripathi et al., 2010; Wu et al., 2000). A more sophisticated physical modeling of crustal event records is thus needed to quantitatively explain the amplitude of T_{pd} measurements in the Pyrenees and to confirm the proposed interpretation of the frequency dependence of T_{pd}.

A part of the dispersion of T_{pd} measurements at a given hypocentral distance could be due to regional variations of scattering along the range. Thus, we propose to explore the spatial variations of envelope broadening after removing the hypocentral dependence described by the regression lines given in Table 1.

5.4. Spatial distribution of T_{pd} in the Pyrenees

5.4.1. Mapping methodology

For the mapping of peak delay times, we follow the method proposed by Takahashi et al. (2007). First, for each frequency band, we remove the hypocentral dependence by computing the peak delay time deviation defined as follows:

$$\Delta\log_{10} T_{pd} = \log_{10} T_{pd}(f) - (A_r(f) + B_r(f)\log_{10} R). \quad (5)$$

As envelope broadening is considered to be the result of multiple forward scattering by inhomogeneities, $\Delta\log_{10} T_{pd}$ may represent the relative strength of accumulated scattering contribution along each ray path. A small $\Delta\log_{10} T_{pd}$ thus implies the absence of strong medium heterogeneities along the ray path from the hypocentre to the station, whereas strong $\Delta\log_{10} T_{pd}$ indicates that a strongly inhomogeneous region is located somewhere along the ray path. For the mapping, we adopt the same approach as the one used for Q_c maps. We only consider 2D spatial variations and we divide the Pyrenean crust into rectangular $0.1^\circ \times 0.1^\circ$ blocks. Next, we allocate the mean values of $\Delta\log_{10} T_{pd}$ to each block. Only blocks that are crossed by at least 5 ray paths are considered. Finally, in each block, we take an average of the mean values over the nearest nine blocks to smooth the spatial variations.

5.4.2. Main characteristics of ΔT_{pd} maps

Fig. 8 shows the distribution of peak delay time deviation in four frequency bands. Blocks with small values of $\Delta\log_{10} T_{pd}$ are indicated by blue colors while blocks of large $\Delta\log_{10} T_{pd}$ values are in red. The top panel shows the ray path density.

First we observe that there is no clear correlation between the $\Delta\log_{10} T_{pd}$ maps and the three main tectonic units. The main feature is an East–West dichotomy in the $\Delta\log_{10} T_{pd}$ spatial distribution. The Western Pyrenees (west to the Adour Fault) exhibit larger $\Delta\log_{10} T_{pd}$ values than the Central and Eastern Pyrenees. It may indicate the presence of strong inhomogeneities in the western part of the range. Indeed, as

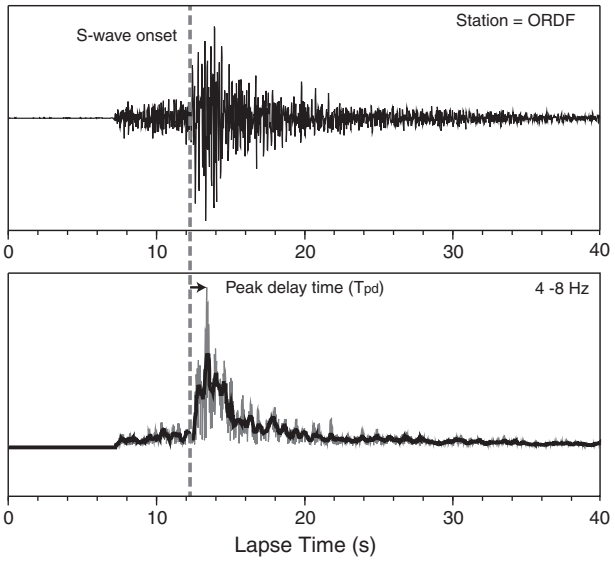

Fig. 6. Example of N–S component velocity seismogram observed at station ORDF (top) and root-mean-square envelope in the 4–8 Hz band (bottom). The thick black line corresponds to the smoothing envelope. The vertical dashed line indicates the S wave onset and the horizontal black arrow represents the peak delay time (T_{pd}).

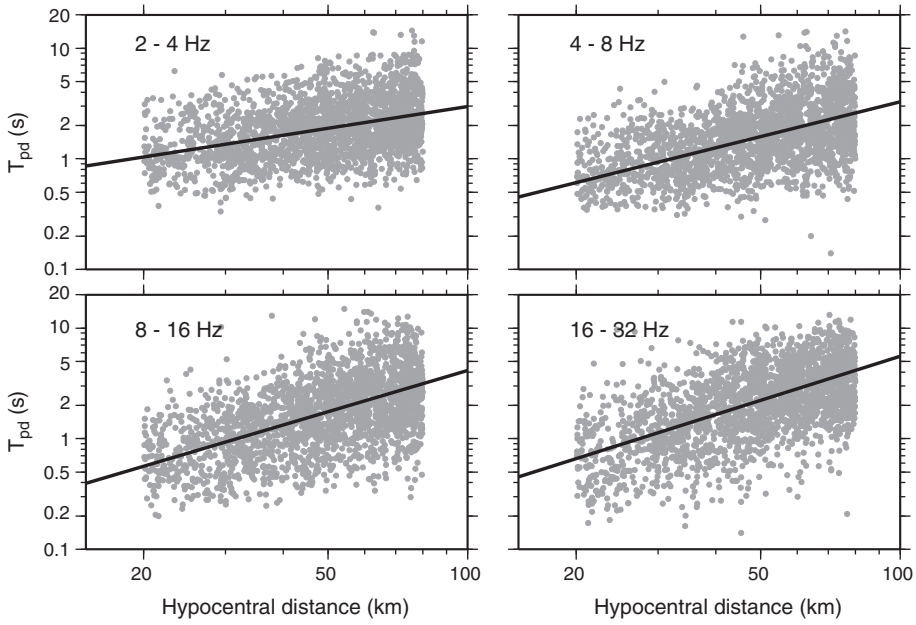

Fig. 7. Logarithmic plot of peak delay times (in seconds) as a function of the hypocentral distance (in kilometers) for crustal S waves in four frequency bands. Gray dots are the data, and black lines are the regression lines: $\log_{10}(T_{pd}) = A_r(f) + B_r(f)\log_{10}R$. The values of coefficient A_r and B_r are listed in Table 1.

absorption and scattering have a competitive effect on the peak delay time, large $\Delta\log_{10}T_{pd}$ values suggest that scattering may be dominant, at least equal, in comparison to absorption at low frequency.

In the Central and Eastern Pyrenees, the Paleozoic Axial Zone and the North Pyrenean Zone show rather small $\Delta\log_{10}T_{pd}$ values in all frequency bands. This feature could be due either to weak scattering or to strong absorption. But Q_c maps show that absorption is low in the PAZ except around the Maladeta Massif (Fig. 8). Thus, scattering in all frequency bands is probably weak on average in the PAZ and NPZ.

Eastern Pyrenees, more particularly to the east of the intermountain basins of Empordà and La Selva, exhibit rather strong $\Delta log_{10}T_{pd}$ values in the 2–4 Hz frequency band. But the amplitude of the peak delay time deviation decreases as frequency increases. This frequency feature may suggest that the crust in the Eastern Pyrenees is richer in small-scale structures than in the Western Pyrenees. However, as absorption becomes stronger as frequency increases, a competition between absorption and scattering may also explain the observed frequency dependence of $\Delta\log_{10}T_{pd}$. In the Eastern Pyrenees, we also observe two high $\Delta\log_{10}T_{pd}$ regions located in the southern thrusts of the Axial zone, close to the compressive faults of Tech and Ribes–Camprodon. These high $\Delta\log_{10}T_{pd}$ anomalies match with regions characterized by strong deformation (Séguret and Choukroune, 1973) and may be related to small scale heterogeneities produced by strong crustal thickening (Vergés et al., 2002).

6. Discussion

In this section we propose to discuss Q_c and $\Delta\log_{10}T_{pd}$ maps in relation with other geophysical and geological observations. Globally, there is no clear correlation between geological structures and attenuation maps in the Pyrenees in all frequency bands. Usually, seismic waves are less attenuated in crystalline materials than in sedimentary ones (Sato et al., 2012). In the Pyrenees, this classical feature is maybe observed only at low frequency. In the next paragraphs, we propose a more detailed discussion.

Table 1
Estimated A_r and B_r parameters with their standard deviation from least-square regression $\log_{10}T_{pd}(f) = A_r(f) + B_r(f)\log_{10}R$ in four frequency bands.

Frequency (Hz)	A_r	SD (A_r)	B_r	SD (B_r)
2.0–4.0	−0.827	0.125	0.649	0.074
4.0–8.0	−1.572	0.125	1.045	0.075
8.0–16.0	−1.859	0.124	1.239	0.075
16.0–32.0	−1.902	0.125	1.323	0.075

6.1. The Eastern Pyrenees

The Eastern Pyrenees, south of the Têt and Tech faults, are characterized by rather small S-wave velocity (Souriau and Granet, 1995; Villaseñor et al., 2007), small (strong) absorption and rather large (small) $\Delta\log_{10}T_{pd}$ values at low (high) frequency. It may indicate that absorption is predominant at high frequency whereas scattering is strong at low frequency. However we cannot quantitatively conclude on the predominance of scattering against absorption (and vice versa). Strong absorption and slightly low velocities suggest a thermal origin of these anomalies and/or the presence of fluids.

We clearly observe that low values of Q_c are mainly found in the Neogene/Quaternary fields characterized by volcanic structures located east of Banyoles–Olot and along the border of the intermountain basin of La Selva (Martí et al., 1992). The Eastern Pyrenees have been strongly affected by the Western Mediterranean extensional phase which has induced a crustal and lithospheric thinning towards the Mediterranean Sea, as revealed by seismic data (Gallart et al., 1981; Mauffret et al., 2001) and gravity data (Ayala et al., 2003; Gunnell et al., 2008; Vergés et al., 2002; Zeyen and Fernàndez, 1994). The late extensional phase was also accompanied by alkaline volcanism. This area is also associated with numerous thermal springs and geothermal anomalies located along faults or at the margins of graben-like structure in the Catalan Coastal Range (Cabal and Fernàndez, 1995; Fernandez and Banda, 1989). In contrast, seismic absorption is smaller west of the volcanic units, in the Ebro Basin, where there is no evidence of thermal springs and where no strong geothermal anomalies have been detected (Fernandez and Banda, 1989). It has been previously shown that volcanic areas in Japan are mainly characterized by strong absorption and scattering (Carcolé and Sato, 2010; Takahashi et al., 2007). The strong absorption observed in the Eastern Pyrenees may be thus related to the late volcanic history with its associated geothermal activity and fluids circulation.

Please cite this article as: Calvet, M., et al., Spatial variations of seismic attenuation and heterogeneity in the Pyrenees: Coda Q and peak delay time analysis, Tectonophysics (2013), http://dx.doi.org/10.1016/j.tecto.2013.08.045

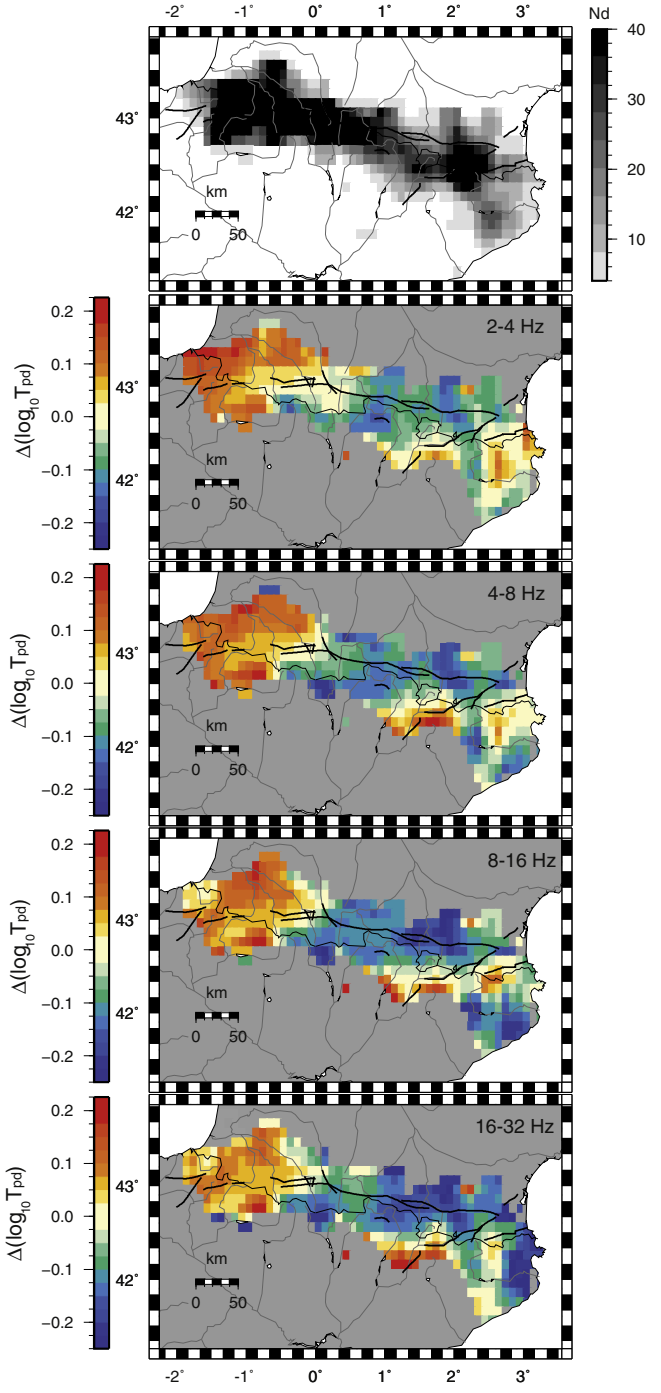

Fig. 8. Distribution of the logarithmic deviation of crustal S-wave peak delay time $\Delta\log_{10}(T_{pd})$ in four frequency bands. We do not consider blocks in which the number of ray paths is less than 5 (gray blocks). The top panel gives the ray path density in all frequency bands. (For interpretation of the references to color in this figure, the reader is referred to the web version of this article.)

6.2. The Western Pyrenees

In the Western Pyrenees, $\Delta log_{10}T_{pd}$ and Q_c maps reveal strong crustal inhomogeneities and strong absorption, respectively.

Analyses of Lg waveforms have also suggested stronger seismic attenuation in this area. Indeed, no crustal phases appear in seismic records of Lg waves when ray paths cross the western part of the range (Chazalon et al., 1993; Sens-Schönfelder et al., 2009). Chazalon et al. (1993) have demonstrated that neither a realistic Moho jump nor a large-scale high-velocity body in the crust can cause such extinction. They speculate that the attenuation of crustal phases may be due to high scattering by small-scale heterogeneities in the Western Pyrenees. This hypothesis has been confirmed by Sens-Schönfelder et al. (2009) who demonstrated that a large-scale body with strong intrinsic absorption and strong scattering may explain the Lg blockage phenomenon. Their best model is characterized by an intrinsic quality factor Q_i about 180 and a scattering quality factor about 340 (at 3 Hz). In the Western Pyrenees, absorption and scattering may be respectively about 4 times and 10 times larger than in the surrounding regions. Our $\Delta\log_{10}T_{pd}$ and Q_c maps show qualitatively that scattering and absorption are on average strong in the Western Pyrenees at low frequency. Even if we do not perform robust inversions, our results are in good agreement with those of Sens-Schönfelder et al. (2009).

The Pau Basin is characterized by rather strong absorption at low frequency (Fig. 5), low-velocities and high V_P/V_S ratio (Daignieres et al., 1981). It could be explained by the presence of oil and gas in the sediments. In the South Pyrenean Zone, the Pamplona Basin is also characterized by low shear wave velocity (Souriau and Granet, 1995; Villaseñor et al., 2007), high V_P/V_S ratio (Fig. 2b), and strong absorption (Fig. 5). However, Q_c varies differently with frequency in the Pau and Pamplona Basins. The difference in the attenuation properties of the two basins may be ascribed to geographical variations either in the chemical composition of sedimentary materials, or in the distribution of fluids, or in the density and connectivity of the fractures (and consequently in fluid circulation) (e.g., Leary, 1995). The Basque and Labourd Massifs are characterized by strong attenuation in all frequency bands. The Mauléon Basin seems to have a distinct behavior with slightly less absorption at high frequency than the surrounding Massifs. Slightly higher V_P/V_S ratio in the Mauléon and Pamplona Basins in comparison to the Basque and Labourd Massifs (see Fig. 2b) suggests the presence of more fluids in the basins than in Paleozoic Massifs. Geographical variations in the fluid contents may also explain a part of the frequency-dependence of absorption in the Mauléon Basin. However, the fluid hypothesis is not compatible with the high seismic velocities observed in this region (Fig. 2a). Alternatively, seismic properties of the Labourd–Mauléon area may be ascribed to the chemical and/or mechanical properties of the crustal materials. Sens-Schönfelder et al. (2009) argue that S-wave absorption in the Western Pyrenees is too strong for crustal materials (Sato et al., 2012). The strong positive Bouguer anomaly observed in the Mauléon–Labourd area (Jammes et al., 2010; Vacher and Souriau, 2001) (see also Fig. 2c) has been interpreted as mantle intrusions which may explain both high seismic velocities and strong absorption.

Peak delay time measurement reveals that scattering is strong in the Western Pyrenees. What is the possible origin of scattering in this area? Close to the surface, it is observed that Cretaceous sediments are locally associated with remnants of lower-crustal and mantle rocks in the Labourd Massifs and the Mauléon Basin. Particularly, the Mauléon Basin contains a number of outcrops, ranging from a few meters to 3 km in diameter, rich in serpentinized mantle peridotites (Jammes et al., 2009; Lagabrielle and Bodinier, 2008). Interestingly, Sens-Schönfelder et al. (2009) obtain a typical size for heterogeneities in the western Pyrenean crust around 800 m. Intrusion of mantle or lower-crustal material is thus a possible mechanism to explain strong seismic scattering in the Western Pyrenees.

6.3. The Central Pyrenees

In all frequency bands, a low-Q_c anomaly (strong absorption) extends from the North Pyrenean Zone to the South Pyrenean Zone. At the same location, small $\Delta\log T_{pd}$ values show that scattering may be smaller than in the Western Pyrenees. East to this low-Q_c anomaly, we also observe that most of the Paleozoic materials are characterized by small absorption (Fig. 5). This East–West dichotomy in the Axial Zone with a transition at the location of the Maladeta Massif cannot be easily explained from tectonic and geological arguments except maybe that most of the Hercynian granitic massifs, the large massifs of gneiss (age

Please cite this article as: Calvet, M., et al., Spatial variations of seismic attenuation and heterogeneity in the Pyrenees: Coda Q and peak delay time analysis, Tectonophysics (2013), http://dx.doi.org/10.1016/j.tecto.2013.08.045

~470 Ma) and the older meta-sediments (Upper Proterozoic to Ordovician) are located in this high-Q_c area (Baudin et al., 2008). We also observe that the Pyrenean seismicity shifts southward at the location of the low-Q_c anomaly. A deep structure in the crust may be at the origin of this attenuation anomaly. Interestingly, an anomalous body has been detected in this area by seismic tomography and analysis of Bouguer anomalies. This high-density and high-velocity crustal body is located south to Saint Gaudens, in the North Pyrenean Zone (see Fig. 2), on the northern border of this Q_c-anomaly. As proposed for the Labourd–Mauléon area, mantle or lower-crustal materials may be at the origin of the observed strong absorption. However, we observe that the Saint Gaudens and Labourd–Mauléon anomalies have a rather distinct seismic behavior. The Saint Gaudens anomaly exhibits smaller absorption, smaller scattering and smaller V_P/V_S ratio than the Labourd–Mauléon one. In both cases, the positive correlation between seismic velocity and attenuation cannot be explained by thermal effects or fluids but suggests that seismic properties may be related to the chemical composition. Variations in the chemical/mineralogical composition of these deep materials may be at the origin of the distinct seismic behavior between the two high density/velocity anomalies. However, from the comparison of gravity and seismic data, Vacher and Souriau (2001) propose a similar mineralogical origin for these two bodies, even if more detailed investigations may be necessary. A part of the difference in absorption between the Saint Gaudens and Labourd–Mauléon anomalies may be also due to a difference in the amount and distribution of mantle materials in the crust.

7. Conclusions

A first attempt at mapping seismic wave attenuation in the Pyrenees has been proposed, based on coda Q and peak delay time analysis in the [1 — 32] Hz frequency band. Q_c maps show that the amplitude and the frequency dependence of attenuation strongly vary along the Pyrenean range. The Paleozoic Axial Zone exhibits mainly lower seismic attenuation than the surrounding regions, except at the longitude of the Maladeta Massif, east of the Adour fault. Seismic waves in the Western Pyrenees, more particularly at the location of the Basques Massifs and the Nappe des Marbres, are strongly attenuated. Similarly the Neogene structures of North-East Catalonia show strong seismic attenuation at high frequency. In addition to coda Q analysis, envelope broadening of high-frequency seismic waves gives complementary information on the origin of seismic attenuation in the Pyrenees, more particularly on the nature of the crustal inhomogeneities. The peak delay time maps highlight a strong East–West dichotomy in the scattering properties of the Pyrenean crust with stronger inhomogeneities in the Western Pyrenees, as previously proposed by Sens-Schönfelder et al. (2009). The Eastern Pyrenees exhibit a likely stronger frequency dependence of the peak delay time than the Western Pyrenees.

The comparison of Q_c and peak delay time maps allows a qualitative discussion about the relative contributions of absorption and scattering to the seismic attenuation in the Pyrenean crust. Anelastic absorption appears to be dominant in the Eastern Pyrenees at high frequency, whereas both absorption and scattering are strong in the Western Pyrenees. We propose that the strong seismic attenuation at the location of the Neogene structures is related to the late volcanic history of the Eastern Pyrenees. In the Western Pyrenees, we argue that the attenuation properties of the crust (strong absorption and scattering) are mainly due to lower-crustal or mantle intrusions related to the complex tectonic history of the region.

Although some correlations have been observed between Q_c, $\Delta\log_{10}T_{pd}$, seismic velocity and V_P/V_S ratio, our findings need to be clarified in several aspect. First, seismic structures in the eastern and western edges of the range are not correctly resolved in the tomography by Souriau and Granet (1995), more particularly the lateral extension of the Labourd–Mauléon high-velocity anomaly. High-resolution crustal tomography may be soon available through to the deployment of the PYROPE and IBERARRAY seismic networks. Second, we only provide coda-Q and peak delay times deviation maps which have been interpreted qualitatively in terms of absorption and scattering. Future works should explore the sensitivity of coda-Q measurements to the lateral and depth variations of absorption. It is clear that our simple mapping approach to Q_c measurements only gives the gross features of the lateral variations of attenuation without any constraint on the depth behavior. Next, we will consider an inversion of the peak delay times, after correction for absorption, in order to better quantify the spatial distribution of the velocity random fluctuations in the Pyrenean crust. Absorption and scattering maps may bring new insights into the structures of the Pyrenees but also offer new elements for interpreting geophysical data (Bouguer anomaly, seismic tomography), seismicity distribution and geological observations. Moreover, such attenuation maps should also significantly improve strong motion prediction in the Pyrenees.

Acknowledgments

The authors would like to thank the different organizations (RSSP, RAP, IGN, IGC, CSIC) that operate temporary and permanent seismological networks in the Pyrenees for making their data available. French seismic data can be collected through the RESIF website (Réseau Sismologique et Géodésique Français — www.resif.fr). The authors are grateful to Marc Calvet, Alexis Rigo, Annie Souriau and Thomas Theunissen for helpful discussions. Haruo Sato and an anonymous reviewer also provided constructive reviews of the manuscript. This work was funded by the European Regional Development Fund (ERDF/FEDER) – POCTEFA program – (SISPyr project), the Agence Nationale de la Recherche (ANR-BLAN 09-0229-000 — project PYROPE) and INSU-CNRS Programs. The temporary network Iber-Array was funded by Consolider-Ingenio 2010 project TOPO-IBERIA (CSD2006-00041).

References

Aki, K., Chouet, B., 1975. Origin of coda waves: source attenuation and scattering effects. J. Geophys. Res. 80, 3322–3342.
Atkinson, G.M., 1993. Notes on ground motion parameters for eastern north America: duration and H/V ratio. Bull. Seismol. Soc. Am. 83, 587–596.
Ayala, C., Torne, M., Pous, J., 2003. The lithosphere–asthenosphere boundary in the western Mediterranean from 3D joint gravity and geoid modeling: tectonic implications. Earth Planet. Sci. Lett. 209 (3), 275–290.
Baudin, T., Barnolas, A., Gil, I., Martin-Alfageme, S., 2008. Carte géologique des Pyrénées à 1/400000. Bureau de Recherches Géologiques et Minières, (BRGM-ITGE).
Cabal, J., Fernàndez, M., 1995. Heat flow and regional uplift at the north-eastern border of the Ebro basin, NE Spain. Geophys. J. Int. 121 (2), 393–403.
Calvet, M., Margerin, L., 2013. Lapse time dependence of coda Q: anisotropic multiple-scattering models and application to Pyrenees. Bull. Seismol. Soc. Am. 3, 1993–2010.
Campillo, M., Plantet, J., 1991. Frequency dependence and spatial distribution of seismic attenuation in France: experimental results and possible interpretations. Phys. Earth Planet. Inter. 67 (1–2), 48–64.
Campillo, M., Plantet, J., Bouchon, M., 1985. Frequency-dependent attenuation in the crust beneath central France from Lg waves: data analysis and numerical modeling. Bull. Seismol. Soc. Am. 75 (5), 1395–1411.
Carcolé, E., Sato, H., 2010. Spatial distribution of scattering loss and intrinsic absorption of short-period S waves in the lithosphere of Japan on the basis of the Multiple Lapse Time Window Analysis of Hi-net data. Geophys. J. Int. 180 (1), 268–290.
Casas, A., Kearey, P., Rivero, L., Adam, C., 1997. Gravity anomaly map of the Pyrenean region and a comparison of the deep geological structure of the western and eastern Pyrenees. Earth Planet. Sci. Lett. 150 (1), 65–78.
Chazalon, A., Campillo, M., Gibson, R., Carreno, E., 1993. Crustal wave propagation anomaly across the Pyrenean range. Comparison between observations and numerical simulations. Geophys. J. Int. 115 (3), 829–838.
Chevrot, S., Cansi, Y., 1996. Source spectra and site-response estimates using the coda of Lg waves in western Europe. Geophys. Res. Lett. 23 (13), 1605–1608.
Chevrot, S., Sylvander, M., Delouis, B., 2011. A preliminary catalog of moment tensors for the Pyrenees. Tectonophysics 150, 239–251.
Choukroune, P., 1992. Tectonic evolution of the Pyrenees. Ann. Rev. Earth Planet. Sci. 20, 143–158.
Choukroune, P., Roure, F., Pinet, B., Team, E., 1990. Main results of the ECORS Pyrenees profile. Tectonophysics 173 (1–4), 411–423.
Correig, A., Mitchell, B., Ortiz, R., 1990. Seismicity and coda Q values in the eastern Pyrenees: first results from the La Cerdanya seismic network. Pure Appl. Geophys. 132 (1), 311–329.
Daignieres, M., Gallart, J., Banda, E., 1981. Lateral variation of the crust in the North Pyrenean Zone. Ann. Geophys. 37 (3), 435–456.

Please cite this article as: Calvet, M., et al., Spatial variations of seismic attenuation and heterogeneity in the Pyrenees: Coda Q and peak delay time analysis, Tectonophysics (2013), http://dx.doi.org/10.1016/j.tecto.2013.08.045

Drouet, S., Souriau, A., Cotton, F., 2005. Attenuation, seismic moments, and site effects for weak-motion events: application to the Pyrenees. Bull. Seismol. Soc. Am. 5, 1731–1748.

Drouet, S., Chevrot, S., Cotton, F., Souriau, A., 2008. Simultaneous inversion of source spectra, attenuation parameters, and site responses: application to the data of the French accelerometric network. Bull. Seismol. Soc. Am. 98 (1), 198–219.

Drouet, S., Cotton, F., Guéguen, P., 2010. vs30, κ, regional attenuation and Mw from accelerograms: application to magnitude 3–5 French earthquakes. Geophys. J. Int. 182 (2), 880–898.

Fehler, M., Hoshiba, M., Sato, H., Obara, K., 1992. Separation of scattering and intrinsic attenuation for the Kanto–Tokai region, Japan, using measurements of s-wave energy versus hypocentral distance. Geophys. J. Int. 108 (3), 787–800.

Fernandez, M., Banda, E., 1989. An approach to the thermal field in northeastern Spain. Tectonophysics 164 (2–4), 259–266.

Fu, L.-Y., Wu, R.-S., Campillo, M., 2002. Energy partition and attenuation of regional phases by random free surface. Bull. Seismol. Soc. Am. 92, 1992–2007.

Gagnepain-Beyneix, J., 1987. Evidence of spatial variations of attenuation in the western Pyrenean range. Geophys. J. Roy. Astron. Soc. 89 (2), 681–704.

Gallart, J., Daignieres, M., Banda, E., Surinach, E., Hirn, A., 1980. The eastern Pyrenean domain: lateral variations at crust–mantle level. Ann. Geophys. 36 (2), 141–158.

Gallart, J., Banda, E., Daignières, M., 1981. Crustal structure of the Paleozoic Axial Zone of the Pyrenees and transition to the North Pyrenean Zone. Ann. Geophys. 3, 457–480.

Gallart, J., Díaz, J., Nercessian, A., Mauffret, A., Dos Reis, T., 2001. The eastern end of the Pyrenees: seismic features at the transition to the NW Mediterranean. Geophys. Res. Lett. 28 (11), 2277–2280.

Gunnell, Y., Zeyen, H., Calvet, M., 2008. Geophysical evidence of a missing lithospheric root beneath the Eastern Pyrenees: consequences for post-orogenic uplift and associated geomorphic signatures. Earth Planet. Sci. Lett. 276 (3–4), 302–313.

Hennino, R., Trégourès, N., Shapiro, N., Margerin, L., Campillo, M., Van Tiggelen, B., Weaver, R., 2001. Observation of equipartition of seismic waves. Phys. Rev. Lett. 86 (15), 3447–3450.

Jammes, S., Manatschal, G., Lavier, L., Masini, E., 2009. Tectonosedimentary evolution related to extreme crustal thinning ahead of a propagating ocean: example of the western Pyrenees. Tectonics 28. http://dx.doi.org/10.1029/2008TC002406 (TC4012).

Jammes, S., Tiberi, C., Manatschal, G., 2010. 3D architecture of a complex transcurrent rift system: the example of the Bay of Biscay–Western Pyrenees. Tectonophysics 1, 210–226.

Lacombe, C., Campillo, M., Paul, A., Margerin, L., 2003. Separation of intrinsic absorption and scattering attenuation from L_g coda decay in central France using acoustic radiative transfer theory. Geophys. J. Int. 154, 417–425.

Lagabrielle, Y., Bodinier, J., 2008. Submarine reworking of exhumed subcontinental mantle rocks: field evidence from the Lherz peridotites, French Pyrenees. Terra Nova 20 (1), 11–21.

Le Pichon, X., Sibuet, J., 1971. Western extension of boundary between European and Iberian plates during the Pyrenean orogeny. Earth Planet. Sci. Lett. 12 (1), 83–88.

Leary, P., 1995. The cause of frequency-dependent seismic absorption in crustal rock. Geophys. J. Int. 122 (1), 143–151.

Margerin, L., Campillo, M., Shapiro, N.M., Tiggelen, B.V., 1999. Residence time of diffuse waves in the crust as a physical interpretation for coda *q*. application to seismograms recorded in Mexico. Geophys. J. Int. 138, 343–352.

Martí, J., Mitjavila, J., Roca, E., Aparicio, A., 1992. Cenozoic magmatism of the Valencia trough (Western Mediterranean): relationship between structural evolution and volcanism. Tectonophysics 203 (1), 145–165.

Mauffret, A., Durand de Grossouvre, B., Tadeu Dos Reis, A., Gorini, C., Nercessian, A., 2001. Structural geometry in the eastern Pyrenees and western Gulf of Lion (Western Mediterranean). J. Struct. Geol 23 (11), 1701–1726.

Mitchell, B., 1995. Anelastic structure and evolution of the continental crust and upper mantle from seismic surface wave attenuation. Rev. Geophys. 33 (4), 441–462.

Mitchell, B., Cong, L., Ekström, G., 2008. A continent-wide map of 1-Hz Lg coda Q variation across Eurasia and its relation to lithospheric evolution. J. Geophys. Res. B04303.

Nocquet, J., Calais, E., 2004. Geodetic measurements of crustal deformation in the Western Mediterranean and Europe. Pure Appl. Geophys. 161 (3), 661–681.

Obara, K., Sato, H., 1995. Regional differences of random inhomogeneities around the volcanic front in the Kanto–Tokai area, Japan, revealed from the broadening of S wave seismogram envelopes. J. Geophys. Res. 100, 2103-2103.

Paasschens, J., 1997. Solution of the time-dependent Boltzmann equation. Phys. Rev. E 56 (1), 1135–1141.

Pacheco, C., Snieder, R., 2005. Time-lapse travel time change of multiply scattered acoustic waves. J. Acoust. Soc. Am. 118, 1300–1310.

Payo, G., Badal, J., Canas, J., Corchete, V., Pujades, L., Serón, F., 1990. Seismic attenuation in Iberia using the coda-Q method. Geophys. J. Int. 103 (1), 135–145.

Petukhin, A.G., Gusev, A.A., 2003. The duration–distance relationship and average envelope shapes of small Kamchatka earthquakes. Pure Appl. Geophys. 160, 171–1743.

Pujades, L., Canas, J., Egozcue, J., Puigvi, M., Gallart, J., Lana, X., Pous, J., Casas, A., 1990. Coda-Q distribution in the Iberian peninsula. Geophys. J. Int. 100 (2), 285–301.

Rigo, A., Souriau, A., Dubos, N., Sylvander, M., Ponsolles, C., 2005. Analysis of the seismicity in the central part of the Pyrenees (France), and tectonic implications. J. Seismol. 9 (2), 211–222.

Romanowicz, B., Mitchell, B., 2007. Q in the earth from crust to core. Treatise on Geophysics 1, 731–774.

Rosenbaum, G., Lister, G., Duboz, C., 2002. Relative motions of Africa, Iberia and Europe during Alpine orogeny. Tectonophysics 359 (1–2), 117–129.

Rossetto, V., Margerin, L., Planès, T., Larose, E., 2011. Locating a weak change using diffuse waves: theoretical approach and inversion procedure. J. Appl. Phys. 109 (3) (034903-034903-11).

Ruiz, M., Gallart, J., Díaz, J., Olivera, C., Pedreira, D., López, C., González-Cortina, J., Pulgar, J., 2006. Seismic activity at the western Pyrenean edge. Tectonophysics 412 (3), 217–235.

Saito, T., Sato, H., Ohtake, M., 2002. Envelope broadening of spherically outgoing waves in three-dimensional random media having power law spectra. J. Geophys. Res. 107 (B5). http://dx.doi.org/10.1029/2001JB000264.

Saito, T., Sato, H., Ohtake, M., Obara, K., 2005. Unified explanation of envelope broadening and maximum-amplitude decay of high-frequency seismograms based on the envelope simulation using the Markov approximation: forearc side of the volcanic front in northeastern Honshu, Japan. J. Geophys. Res. 110. http://dx.doi.org/10.1029/2004JB003225 (B01304).

Sato, H., 1989. Broadening of seismogram envelopes in the randomly inhomogeneous lithosphere based on the parabolic approximation: Southeastern Honshu, Japan. J. Geophys. Res. 94, 17–735.

Sato, H., Fehler, M.C., Maeda, T., 2012. Seismic wave propagation and scattering in the heterogeneous Earth, 2nd edn. Springer, Berlin.

Séguret, Choukroune, P., 1973. Carte structurale des Pyrénées, Université des Sciences et Techniques du Languedoc. Laboratoire de géologie structurale.

Sens-Schönfelder, C., Margerin, L., Campillo, M., 2009. Laterally heterogeneous scattering explains Lg blockage in the Pyrenees. J. Geophys. Res. 114. http://dx.doi.org/10.1029/2008JB006107 (B07309).

Souriau, A., Granet, M., 1995. A tomographic study of the lithosphere beneath the Pyrenees from local and teleseismic data. J. Geophys. Res. 100 (B9), 18117–18134.

Souriau, A., Pauchet, H., 1998. A new synthesis of Pyrenean seismicity and its tectonic implications. Tectonophysics 290 (3–4), 221–244.

Souriau, A., Sylvander, M., Rigo, A., Fels, J., Douchain, J., Ponsolles, C., 2001. Sismotectonique des Pyrénées; principales contraintes sismologiques. Bull. Soc. Geol. Fr. 172 (1), 25–39.

Souriau, A., Chaljub, E., Cornou, C., Margerin, L., Calvet, M., Maury, J., Wathelet, M., Grimaud, F., Ponsolles, C., Péquegnat, C., et al., 2011. Multimethod characterization of the French-Pyrenean valley of Bagnères-de-Bigorre for seismic-hazard evaluation: observations and models. Bull. Seismol. Soc. Am. 101 (4), 1912–1937.

Srivastava, S., Sibuet, J., Cande, S., Roest, W., Reid, I., 2000. Magnetic evidence for slow seafloor spreading during the formation of the Newfoundland and Iberian margins. Earth Planet. Sci. Lett. 182 (1), 61–76.

Takahashi, T., Sato, H., Nishimura, T., Obara, K., 2007. Strong inhomogeneity beneath Quaternary volcanoes revealed from the peak delay analysis of S-wave seismograms of microearthquakes in northeastern Japan. Geophys. J. Int. 168 (1), 90–99.

Takahashi, T., Sato, H., Nishimura, T., Obara, K., 2009. Tomographic inversion of the peak delay times to reveal random velocity fluctuations in the lithosphere: method and application to northeastern Japan. Geophys. J. Int. 178 (3), 1437–1455.

Tripathi, J.N., Sato, H., Yamamoto, M., 2010. Envelope broadening characteristics of crustal earthquakes in northeastern Honshu, Japan. Geophys. J. Int. 1182, 988–1000.

Vacher, P., Souriau, A., 2001. A three-dimensional model of the Pyrenean deep structure based on gravity modelling, seismic images and petrological constraints. Geophys. J. Int. 145 (2), 460–470.

Vargas, C., Ugalde, A., Pujades, L., Canas, J., 2004. Spatial variation of coda wave attenuation in northwestern Colombia. Geophys. J. Int. 158 (2), 609–624.

Vergés, J., Fernàndez, M., Martínez, A., 2002. The Pyrenean orogen: pre-, syn-, and post-collisional evolution. J. Virtual Explor. 8, 57–76.

Villaseñor, A., Yang, Y., Ritzwoller, M., Gallart, J., 2007. Ambient noise surface wave tomography of the Iberian Peninsula: implications for shallow seismic structure. Geophys. Res. Lett. 34 (11). http://dx.doi.org/10.1029/2007GL030164 (L11304).

Vissers, R., Meijer, P., 2012. Mesozoic rotation of Iberia: subduction in the Pyrenees? Earth Sci. Rev. 110, 93–110.

Wu, R.-S., Jin, S., Xie, X., 2000. Seismic wave propagation and scattering in heterogeneous crustal waveguides using screen propagators: I SH waves. Bull. Seismol. Soc. Am. 90 (2), 401–413.

Zeyen, H., Fernàndez, M., 1994. Integrated lithospheric modeling combining thermal, gravity, and local isostasy analysis: application to the NE Spanish Geotransect. J. Geophys. Res. 99 (B9), 18089–18102.

Please cite this article as: Calvet, M., et al., Spatial variations of seismic attenuation and heterogeneity in the Pyrenees: Coda Q and peak delay time analysis, Tectonophysics (2013), http://dx.doi.org/10.1016/j.tecto.2013.08.045